Steel and Composite Structures, *Vol. 15, No. 2 (2013) 221-245*
DOI: http://dx.doi.org/10.12989/scs.2013.15.2.221

Thermo-mechanical bending response with stretching effect of functionally graded sandwich plates using a novel shear deformation theory

Hayat Saidi[1], Mohammed Sid Ahmed Houari[2], Abdelouahed Tounsi[*1,2,3] and El Abbas Adda Bedia[1]

[1] Laboratoire des Matériaux et Hydrologie, Université de Sidi Bel Abbes, Faculté de Technologie, BP 89 Cité Ben M'hidi 22000 Sidi Bel Abbes, Algérie
[2] Laboratoire des Structures et Matériaux Avancés dans le Génie Civil et Travaux Publics, Université de Sidi Bel Abbes, Faculté de Technologie, BP 89 Cité Ben M'hidi 22000 Sidi Bel Abbes, Algérie
[3] Département de Génie Civil, Faculté de Technologie, Université Sidi Bel Abbes, Algérie

(Received January 29, 2013, Revised June 11, 2013, Accepted July 11, 2013)

Abstract. This paper presents an analytical solution to the thermomechanical bending analysis of functionally graded sandwich plates by using a new hyperbolic shear deformation theory in which the stretching effect is included. The modulus of elasticity of plates is assumed to vary according to a power law distribution in terms of the volume fractions of the constituents. The core layer is still homogeneous and made of an isotropic ceramic material. The effects of functionally graded material (FGM) layer thickness, volume fraction index, layer thickness ratio, thickness ratio and aspect ratio on the deflections and stresses of functionally graded sandwich plates are investigated.

Keywords: plate; thermomechanical; analytical modelling; functionally graded material; stretching effect

1. Introduction

Functionally graded materials (FGMs) are microscopically inhomogeneous composites usually made of a mixture of metals and ceramics. By gradually varying the volume fraction of their constituents, it can be achieved that the effective properties of FGMs exhibit a smooth and continuous change from one surface to another, thus eliminating interface problems and mitigating thermal stress concentrations. Due to the high heat resistance, FGMs are used as structural components operating in ultrahigh-temperature environments and subjected to extremely high thermal gradients, such as aircraft, space vehicles, nuclear plants, and other engineering applications. Indeed, the thermo-mechanical deformation of functionally grade (FG) structures have attracted the attention of many researchers in the past few years in different engineering applications which include design of aerospace structures, heat engine components and nuclear power plants etc.

*Corresponding author, Professor, E-mail: tou_abdel@yahoo.com

http://www.techno-press.org/?journal=scs&subpage=8 ISSN: 1229-9367 (Print), 1598-6233 (Online)

The assessment of thermo-mechanical deformation behavior of functionally graded plate structures considerably depends on the plate model kinematics. A number of plate theories are available to analyze the deformations of composite plates. The foremost constraint of using the classical Kirchhoff plate theory (CPT) is that it ignores transverse shear effects and consequently provides reasonable results for relatively thin plates. However, in thick and moderately thick plates, the transverse shear strains have to be taken into account. There are numerous plate theories that include these strains (Reissner 1945, Mindlin 1951). These theories are often called the first order shear deformation theory (FSDT) and a shear-correction factor is needed to eliminate the problem of a constant transverse shear stress distribution. Higher order shear deformation theories (HSDTs) were developed to improve the analysis of structure responses and extensively used by many researchers (Lo *et al*. 1977, Levinson 1980, Murthy 1981, Reddy 1984, Bert 1984, Matsunaga 2000, Karama *et al*. 2003, Şimşek 2009, 2010, Zenkour and Alghamdi 2010, Atmane *et al*. 2010).

Reddy (2000) presented the third-order shear deformation theory (TSDT) in which the transverse shear stresses are represented as quadratic through the thickness and consequently it requires no shear correction factors and developed the associated finite element model. Cheng and Batra (2000a) have related the deflections of a simply supported FG polygonal plate given by the first-order shear deformation theory and a third-order shear deformation theory to that of an equivalent homogeneous Kirchhoff plate. Cheng and Batra (2000b) have also presented results for the buckling and steady state vibrations of a simply supported FG polygonal plate based on Reddy's plate theory. Analytical 3D solutions for plates are useful since they provide benchmark results to assess the accuracy of various 2D plate theories and finite element formulations. Cheng and Batra (2000c) have also used the method of asymptotic expansion to study the 3D thermoelastic deformations of an FG elliptic plate. Vel and Batra (2002) have presented an exact 3D solution for the thermoelastic deformation of FG simply supported plates of finite dimensions. A generalized refined plate theory is used to investigate the cylindrical bending behavior of FG plates by Bian *et al*. (2005) and a laminate model is employed to approximate the FG plate by assuming material homogeneity within each thin layer. Lü *et al*. (2009a) presented a semi-analytical 3-D elasticity solutions for orthotropic multi-directional functionally graded plates using the differential quadrature method (DQM) based on the state-space formalism. Lü *et al*. (2009b) studied the free vibration of FG thick plates on Pasternak foundation using 3-D exact solutions. Ying *et al*. (2009) used a semi-analytical method to study thermal deformations of FG thick plates and the analysis is directly based on the 3-D theory of elasticity. A two-dimensional theory of elasticity is used together with the state space formulation by Lim *et al*. (2009) to investigate the temperature-dependent in-plane vibration of FG circular arches. Zhang *et al*. (2003) developed an exact solution for thermal stresses around a hole in a functionally graded plate. An asymptotic solution approach for free vibration of simply supported FG circular arches is developed in the framework of the two-dimensional theory of elasticity by Zeng *et al*. (2012). A two-dimensional global higher-order deformation theory has been employed by Matsunaga (2009) for thermal buckling of FG plates. Bouderba *et al*. (2013) studied the thermomechanical bending response of FG plates resting on elastic foundations using a refined trigonometric shear deformation theory. Yaghoobi and Yaghoobi (2013) proposed an analytical investigation on the buckling analysis of symmetric sandwich plates with FG face sheets resting on an elastic foundation based on the first-order shear deformation plate theory and subjected to mechanical, thermal and thermo-mechanical loads. Tounsi and his co-works (Hadji *et al*. 2011, Houari *et al*. 2011, Abdelaziz *et al*. 2011, Merdaci *et al*. 2011, Bourada *et al*. 2012, Tounsi *et al*. 2013, Hamidi *et al*. 2013) developed new refined plate theories for bending response, buckling and free vibration

of simply supported FG sandwich plate with only four unknown functions was developed.

In the present paper, an analytical solution to the thermomechanical bending analysis of functionally graded sandwich plates is developed using a new hyperbolic shear deformation theory including the so-called "stretching effect". The sandwich plate faces are assumed to have isotropic, two-constituent (metal-ceramic) material distribution through the thickness, and the modulus of elasticity, Poisson's ratio, and thermal expansion coefficient of the faces are assumed to vary according to a power law distribution in terms of the volume fractions of the constituents. The core layer is still homogeneous and made of an isotropic ceramic material. Numerical results for deflections and stresses are investigated.

2. Theoretical formulation

Consider a flat sandwich plate composed of three (metal-ceramic, ceramic, ceramic-metal) layers as shown in Fig. 1. Rectangular Cartesian coordinates (x, y, z) are used to describe infinitesimal deformations of a three-layer sandwich elastic plate occupying the region $[0,a] \times [0,b] \times [-h/2, h/2]$ in the unstressed reference configuration. The mid-plane is defined by $z = 0$ and its external bounding planes being defined by $z = \pm h/2$. The face layers of the sandwich plate are made of an isotropic material with material properties varying smoothly in the z (thickness) direction only. The core layer is made of an isotropic homogeneous material. The vertical positions of the bottom surface, the two interfaces between the core and faces layers, and the top surface are denoted, respectively, by $h_0 = -h/2$, h_1, h_2 and $h_3 = h/2$. The total thickness of the FG plate is h, where $h = t_c + t_{FGM}$ and $t_c = h_2 - h_1$. t_c and t_{FGM} are the layer thickness of the core and all-FGM layers, respectively.

The effective material properties for each layer, like Young's modulus, Poisson's ratio and thermal expansion coefficient, can be expressed as

$$P^{(n)}(z) = P_m + \left(P_c - P_m\right)V^{(n)} \tag{1}$$

where $P^{(n)}$ is the effective material property of FGM of layer n. P_m and P_c denote the property of the bottom and top faces of layer 1 ($h_0 \le z \le h_1$), respectively, and vice versa for layer 3 ($h_2 \le z \le h_3$)

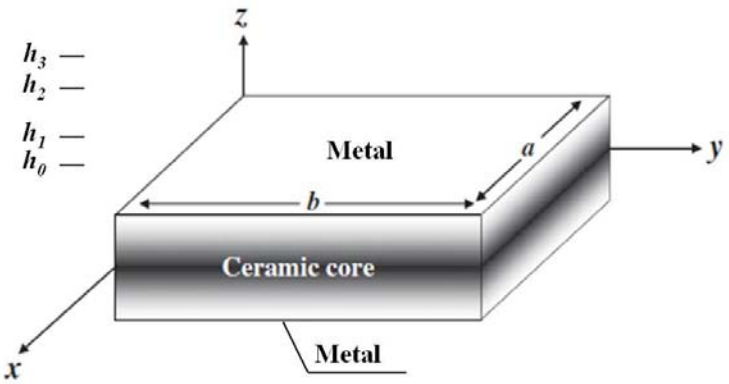

Fig. 1 Geometry of the FGM sandwich plate

depending on the volume fraction $V^{(n)}$ (n = 1, 2, 3). Note that P_m and P_c are, respectively, the corresponding properties of the metal and ceramic of the FG sandwich plate. The volume fraction $V^{(n)}$ of the FGMs is assumed to obey a power-law function along the thickness direction (Houari *et al*. 2011).

$$V^{(1)} = \left(\frac{z - h_0}{h_1 - h_0} \right)^k, \quad z \in [h_0, h_1] \tag{2a}$$

$$V^{(2)} = 1, \quad z \in [h_1, h_2] \tag{2b}$$

$$V^{(3)} = \left(\frac{z - h_3}{h_2 - h_3} \right)^k, \quad z \in [h_2, h_3] \tag{2c}$$

where k is the volume fraction exponent, which takes values greater than or equals to zero. The core layer is independent of the value of k which is a fully ceramic layer. However, the value of k equal to zero represents a fully ceramic plate. The above power-law assumption given in Eqs. (2a) and (2c) reflects a simple rule of mixtures used to obtain the effective properties of the metal-ceramic and ceramic-metal plate faces (see Fig. 1). Note that the volume fraction of the metal is high near the bottom and top surfaces of the plate, and that of ceramic is high near the interfaces.

This paper presents a new hyperbolic shear deformation theory for FG sandwich plates, including the stretching of the thickness. The new displacement field is described in the following equations

$$u = u_0(x, y) - z \frac{\partial w_0}{\partial x} + f(z)\, \theta_x \tag{3a}$$

$$v = v_0(x, y) - z \frac{\partial w_0}{\partial y} + f(z)\, \theta_y \tag{3b}$$

$$w = w_0(x, y) + f'(z)\, \theta_z \tag{3c}$$

with

$$f(z) = \frac{\cosh(\pi/2)}{\left[\cosh(\pi/2) - 1\right]} z - \frac{(h/\pi)\sinh\left(\frac{\pi}{h} z\right)}{\left[\cosh(\pi/2) - 1\right]} \tag{3d}$$

where, u, v, w are displacements in the x, y, z directions, u_0, v_0 and w_0 are midplane displacements, θ_x, θ_y and θ_z rotations of the yz, xz, and xy planes due to bending, respectively. $f(z)$ represents shape function determining the distribution of the transverse shear strains and stresses along the thickness and $f'(z) = \partial f(z) / \partial z$.

The displacement field of the classical thin plate theory (CPT) is obtained easily by setting $f(z) = 0$ and $\theta_z = 0$. The displacement of the first shear deformation theory (FSDT) is obtained by setting $f(z) = 0$ and $\theta_z = 0$. Also, the displacement of third shear deformation theory (TSDT) of Reddy (1984) is obtained by setting

$$f(z) = z\left(1 - \frac{4z^2}{3h^2}\right) \quad \text{and} \quad \theta_z = 0 \tag{4a}$$

The sinusoidal shear deformation theory (SSDT) of Zenkour and Alghamdi (2010) is obtained by setting

$$f(z)=\frac{h}{\pi}\sin\left(\frac{\pi z}{h}\right) \quad \text{and} \quad \theta_z=0 \tag{4b}$$

In addition, the exponential shear deformation theory (ESDT) of Karama *et al*. (2003) is obtained by setting

$$f(z)=ze^{-2(z/h)^2} \quad \text{and} \quad \theta_z=0 \tag{4c}$$

In addition, the displacement field of the hyperbolic shear deformation plate theory (HSDT) of Atmane *et al*. (2010) is obtained by setting

$$f(z)=\frac{\cosh(\pi/2)}{\left[\cosh(\pi/2)-1\right]}z-\frac{(h/\pi)\sinh\left(\frac{\pi}{h}z\right)}{\left[\cosh(\pi/2)-1\right]} \quad \text{and} \quad \theta_z=0 \tag{4d}$$

The displacement field of the present refined hyperbolic shear deformation theory (RHSDT) which includes the stretching of the thickness with $\theta_z\neq 0$ is simplified by enforcing traction-free boundary conditions at the plate faces. It contains one dependent unknown more than that in the first-, third-, exponential- and sinusoidal shear deformation theories. No transverse shear correction factors are needed for TSDT, SSDT, ESDPT, HSDT and RHSDT because a correct representation of the transverse shearing strain is given. In addition, the effect of normal deformation is included in the present theory.

In the derivation of the necessary equations, small strains are assumed (i.e., displacements and rotations are small, and obey Hooke's law). The linear strain expressions derived from the displacement model of Eqs. (3a-c), valid for thin, moderately thick and thick plate under consideration are as follows

$$\begin{Bmatrix}\varepsilon_x\\ \varepsilon_y\\ \gamma_{xy}\end{Bmatrix}=\begin{Bmatrix}\varepsilon_x^0\\ \varepsilon_y^0\\ \gamma_{xy}^0\end{Bmatrix}+z\begin{Bmatrix}k_x\\ k_y\\ k_{xy}\end{Bmatrix}+f(z)\begin{Bmatrix}\eta_x\\ \eta_y\\ \eta_{xy}\end{Bmatrix} \tag{5a}$$

$$\varepsilon_z=f''(z)\varepsilon_z^0 \tag{5b}$$

$$\begin{Bmatrix}\gamma_{yz}\\ \gamma_{xz}\end{Bmatrix}=f'(z)\begin{Bmatrix}\gamma_{yz}^0\\ \gamma_{xz}^0\end{Bmatrix} \tag{5c}$$

where

$$\begin{gathered}\varepsilon_x^0=\frac{\partial u_0}{\partial x},\ \varepsilon_y^0=\frac{\partial v_0}{\partial y},\ \varepsilon_z^0=\theta_z,\ \gamma_{yz}^0=\left(\theta_y+\frac{\partial\theta_z}{\partial y}\right),\ \gamma_{xz}^0=\left(\theta_x+\frac{\partial\theta_z}{\partial x}\right),\\ \gamma_{xy}^0=\frac{\partial u_0}{\partial y}+\frac{\partial v_0}{\partial x},\ k_x=-\frac{\partial^2 w_0}{\partial x^2},\ k_y=-\frac{\partial^2 w_0}{\partial y^2},\ k_{xy}=-2\frac{\partial^2 w_0}{\partial x\partial y},\\ \eta_x=\frac{\partial\theta_x}{\partial x},\ \eta_y=\frac{\partial\theta_y}{\partial y},\ \eta_{xy}=\frac{\partial\theta_x}{\partial y}+\frac{\partial\theta_y}{\partial x}\end{gathered} \tag{6}$$

The linear constitutive relations are given as

$$\begin{Bmatrix} \sigma_x \\ \sigma_y \\ \sigma_z \\ \tau_{yz} \\ \tau_{xz} \\ \tau_{xy} \end{Bmatrix} = \begin{bmatrix} Q_{11} & Q_{12} & Q_{13} & 0 & 0 & 0 \\ Q_{12} & Q_{22} & Q_{23} & 0 & 0 & 0 \\ Q_{13} & Q_{23} & Q_{33} & 0 & 0 & 0 \\ 0 & 0 & 0 & Q_{44} & 0 & 0 \\ 0 & 0 & 0 & 0 & Q_{55} & 0 \\ 0 & 0 & 0 & 0 & 0 & Q_{66} \end{bmatrix} \begin{Bmatrix} \varepsilon_x \\ \varepsilon_y \\ \varepsilon_z \\ \gamma_{yz} \\ \gamma_{xz} \\ \gamma_{xy} \end{Bmatrix} \tag{7}$$

where (σ_x, σ_y, σ_z, τ_{yz}, τ_{xz}, τ_{xy}) and (ε_x, ε_y, ε_z, γ_{yz}, γ_{xz}, γ_{xy}) are the stress and strain components, respectively. Using the material properties defined in Eq. (1), stiffness coefficients, Q_{ij}, can be expressed as

$$Q_{11} = Q_{22} = Q_{33} = \frac{E(z)}{1-\nu^2}, \tag{8a}$$

$$Q_{12} = Q_{13} = Q_{23} = \frac{\nu\, E(z)}{1-\nu^2}, \tag{8b}$$

$$Q_{44} = Q_{55} = Q_{66} = \frac{E(z)}{2(1+\nu)}, \tag{8c}$$

Considering the static version of the principle of virtual work, the following expressions can be obtained

$$\int_{-h/2}^{h/2} \int_{\Omega} \left[\sigma_x \delta\, \varepsilon_x + \sigma_y \delta\, \varepsilon_y + \sigma_z \delta\, \varepsilon_z + \tau_{xy} \delta\, \gamma_{xy} + \tau_{yz} \delta\, \gamma_{yz} + \tau_{xz} \delta\, \gamma_{xz}\right] d\Omega\, dz - \int_{\Omega} q \delta\, w d\Omega = 0 \tag{9}$$

where Ω is the top surface and q is the distributed transverse load.

Substituting Eqs. (3), (5) and (7) into Eq. (9) and integrating through the thickness of the plate, Eq. (9) can be rewritten as

$$\begin{aligned} \int_{\Omega} \Big[& N_x \delta\, \varepsilon_x^0 + N_y \delta\, \varepsilon_y^0 + N_z \delta\, \varepsilon_z^0 + N_{xy} \delta\, \gamma_{xy}^0 + M_x \delta\, k_x + M_y \delta\, k_y + M_{xy} \delta\, k_{xy} \\ & + S_x \delta\, \eta_x + S_y \delta\, \eta_y + S_{xy} \delta\, \eta_{xy} + Q_{yz} \delta\, \gamma_{yz} + Q_{xz} \delta\, \gamma_{xz} - q \delta\, w \Big] d\Omega = 0 \end{aligned} \tag{10}$$

where

$$\begin{Bmatrix} N_x, & N_y, & N_{xy} \\ M_x, & M_y, & M_{xy} \\ S_x, & S_y, & S_{xy} \end{Bmatrix} = \sum_{n=1}^{3} \int_{h_n}^{h_{n+1}} \left(\sigma_x, \sigma_y, \tau_{xy}\right)^{(n)} \begin{Bmatrix} 1 \\ z \\ f(z) \end{Bmatrix} dz, \tag{11a}$$

$$N_z = \sum_{n=1}^{3} \int_{h_n}^{h_{n+1}} \sigma_z^{(n)} f''(z) dz, \tag{11b}$$

$$\left(Q_{xz}, Q_{yz}\right) = \sum_{n=1}^{3} \int_{h_n}^{h_{n+1}} \left(\tau_{xz}, \tau_{yz}\right)^{(n)} f'(z) dz. \tag{11c}$$

where h_{n+1} and h_n are the top and bottom z-coordinates of the nth layer.

The governing equations of equilibrium can be derived from Eq. (10) by integrating the displacement gradients by parts and setting the coefficients δu_0, δv_0, δw_0, $\delta\theta_x$, $\delta\theta_y$ and $\delta\theta_z$ to zero separately. Thus one can obtain the equilibrium equations associated with the present unified shear deformation theory

$$\frac{\partial N_x}{\partial x}+\frac{\partial N_{xy}}{\partial y}=0 \tag{12a}$$

$$\frac{\partial N_{xy}}{\partial x}+\frac{\partial N_y}{\partial y}=0 \tag{12b}$$

$$\frac{\partial^2 M_x}{\partial x^2}+2\frac{\partial^2 M_{xy}}{\partial x\partial y}+\frac{\partial^2 M_y}{\partial y^2}+q=0 \tag{12c}$$

$$\frac{\partial S_x}{\partial x}+\frac{\partial S_{xy}}{\partial y}-Q_{xz}=0 \tag{12d}$$

$$\frac{\partial S_{xy}}{\partial x}+\frac{\partial S_y}{\partial y}-Q_{yz}=0 \tag{12e}$$

$$\frac{\partial Q_{xz}}{\partial x}+\frac{\partial Q_{yz}}{\partial y}-N_z=0 \tag{12f}$$

Using Eq. (7) in Eq. (11), the stress resultants of a sandwich plate made up of three layers can be related to the total strains by

$$\begin{Bmatrix} N \\ M \\ S \end{Bmatrix}=\begin{bmatrix} A & B & B^a \\ B & D & D^a \\ B^a & D^a & F^a \end{bmatrix}\begin{Bmatrix} \varepsilon \\ k \\ \eta \end{Bmatrix}+\delta_{xy}\begin{bmatrix} L \\ L^a \\ R \end{bmatrix}\varepsilon_z^0-\begin{Bmatrix} N^T \\ M^T \\ S^T \end{Bmatrix},\quad Q=A^a\gamma \tag{13a}$$

$$N_z=R^a\theta_z+L\left(\varepsilon_x^0+\varepsilon_y^0\right)+L^a\left(k_x+k_y\right)+R\left(\eta_x+\eta_y\right)-N_z^T, \tag{13b}$$

where δ_{xy} is the Kronecker's delta, and

$$N=\left\{N_x,N_y,N_{xy}\right\}^t,\quad M=\left\{M_x,M_y,M_{xy}\right\}^t,\quad S=\left\{S_x,S_y,S_{xy}\right\}^t \tag{14a}$$

$$N^T=\left\{N_x^T,N_y^T,0\right\}^t,\quad M^T=\left\{M_x^T,M_y^T,0\right\}^t,\quad S^T=\left\{S_x^T,S_y^T,0\right\}^t \tag{14b}$$

$$\varepsilon=\left\{\varepsilon_x^0,\varepsilon_y^0,\gamma_{xy}^0\right\}^t,\quad k=\left\{k_x,k_y,k_{xy}\right\}^t,\quad \eta=\left\{\eta_x,\eta_y,\eta_{xy}\right\}^t \tag{14c}$$

$$A=\begin{bmatrix} A_{11} & A_{12} & 0 \\ A_{12} & A_{22} & 0 \\ 0 & 0 & A_{66} \end{bmatrix},\quad B=\begin{bmatrix} B_{11} & B_{12} & 0 \\ B_{12} & B_{22} & 0 \\ 0 & 0 & B_{66} \end{bmatrix},\quad D=\begin{bmatrix} D_{11} & D_{12} & 0 \\ D_{12} & D_{22} & 0 \\ 0 & 0 & D_{66} \end{bmatrix} \tag{14d}$$

$$B^a = \begin{bmatrix} B_{11}^a & B_{12}^a & 0 \\ B_{12}^a & B_{22}^a & 0 \\ 0 & 0 & B_{66}^a \end{bmatrix}, \quad D^a = \begin{bmatrix} D_{11}^a & D_{12}^a & 0 \\ D_{12}^a & D_{22}^a & 0 \\ 0 & 0 & D_{66}^a \end{bmatrix}, \quad F^a = \begin{bmatrix} F_{11}^a & F_{12}^a & 0 \\ F_{12}^a & F_{22}^a & 0 \\ 0 & 0 & F_{66}^a \end{bmatrix} \tag{14e}$$

$$Q = \left\{Q_{xz}, Q_{yz}\right\}^t, \quad \gamma = \left\{\gamma_{xz}^0, \gamma_{yz}^0\right\}^t, \quad A^a = \begin{bmatrix} A_{44}^a & 0 \\ 0 & A_{55}^a \end{bmatrix} \tag{14f}$$

where N and M are the basic components of stress resultants and stress couples, S are additional stress couples associated with the transverse shear effects, Q and N_z are transverse and normal shear stress resultants. Note that the superscript t denotes the transpose of the given vector. The stiffness coefficients A_{ij} and B_{ij}, … etc., are defined as

$$\begin{Bmatrix} A_{11} & B_{11} & D_{11} & B_{11}^a & D_{11}^a & F_{11}^a \\ A_{12} & B_{12} & D_{12} & B_{12}^a & D_{12}^a & F_{12}^a \\ A_{66} & B_{66} & D_{66} & B_{66}^a & D_{66}^a & F_{66}^a \end{Bmatrix} = \sum_{n=1}^{3} \int_{h_n}^{h_{n+1}} Q_{11}^{(n)} \left(1, z, z^2, f(z), z\, f(z), f^2(z)\right) \begin{Bmatrix} 1 \\ \nu^{(n)} \\ \dfrac{1-\nu^{(n)}}{2} \end{Bmatrix} dz \tag{15a}$$

and

$$\left(A_{22}, B_{22}, D_{22}, B_{22}^a, D_{22}^a, F_{22}^a\right) = \left(A_{11}, B_{11}, D_{11}, B_{11}^a, D_{11}^a, F_{11}^a\right), \quad Q_{11}^{(n)} = \frac{E(z)}{1-\upsilon^2} \tag{15b}$$

$$\begin{Bmatrix} L \\ L^a \\ R \\ R^a \end{Bmatrix} = \sum_{n=1}^{3} \int_{h_n}^{h_{n+1}} Q_{11}^{(n)} \begin{Bmatrix} \nu^{(n)} \\ \nu^{(n)} z \\ \nu^{(n)} f(z) \\ f''(z) \end{Bmatrix} f''(z) dz \tag{15c}$$

$$A_{44}^a = A_{55}^a = \sum_{n=1}^{3} \int_{h_n}^{h_{n+1}} \frac{E(z)}{2(1+\nu)} \left[f'(z)\right]^2 dz, \tag{15d}$$

The stress and moment resultants, $N_x^T = N_y^T$, $M_x^T = M_y^T$, $S_x^T = S_y^T$ and N_z^T due to thermal loading are defined by

$$\begin{Bmatrix} N_x^T \\ M_x^T \\ S_x^T \\ N_z^T \end{Bmatrix} = \sum_{n=1}^{3} \int_{h_n}^{h_{n+1}} \frac{E(z)}{1-\nu^2} (1+2\nu) \alpha(z) T \begin{Bmatrix} 1 \\ z \\ f(z) \\ f''(z) \end{Bmatrix} dz, \tag{16}$$

The temperature field variation through the thickness is assumed to be

$$T(x, y, z) = T_1(x, y) + \frac{z}{h} T_2(x, y) + \frac{f(z)}{h} T_3(x, y), \tag{17}$$

where T_1, T_2 and T_3 are thermal loads.

Substituting from Eq. (13) into Eq. (12), we obtain the following equation

$$\begin{aligned} &A_{11}d_{11}u_0 + A_{66}d_{22}u_0 + (A_{12}+A_{66})d_{12}v_0 - B_{11}d_{111}w_0 - (B_{12}+2B_{66})d_{122}w_0 \\ &+ (B^a_{12}+B^a_{66})d_{12}\theta_y + B^a_{66}d_{22}\theta_x + B^a_{11}d_{11}\theta_x + Ld_1\theta_z = p_1, \end{aligned} \tag{18a}$$

$$\begin{aligned} &A_{22}d_{22}v_0 + A_{66}d_{11}v_0 + (A_{12}+A_{66})d_{12}u_0 - B_{22}d_{222}w_0 - (B_{12}+2B_{66})d_{112}w_0 \\ &+ (B^a_{12}+B^a_{66})d_{12}\theta_x + B^a_{66}d_{11}\theta_y + B^a_{22}d_{22}\theta_y + Ld_2\theta_z = p_2, \end{aligned} \tag{18b}$$

$$\begin{aligned} &-B_{11}d_{111}u_0 - (B_{12}+2B_{66})d_{122}u_0 - (B_{12}+2B_{66})d_{112}v_0 - B_{22}d_{222}v_0 \\ &+ D_{11}d_{1111}w_0 + 2(D_{12}+2D_{66})d_{1122}w_0 + D_{22}d_{2222}w_0 - D^a_{11}d_{111}\theta_x \\ &-(D^a_{12}+2D^a_{66})d_{122}\theta_w - (D^a_{12}+2D^a_{66})d_{112}\theta_y - D^a_{22}d_{222}\theta_y - L^a(d_{11}\theta_z + d_{22}\theta_z) = p_3, \end{aligned} \tag{18c}$$

$$\begin{aligned} &B^a_{11}d_{11}u_0 + B^a_{66}d_{22}u_0 + (B^a_{12}+B^a_{66})d_{12}v_0 - D^a_{11}d_{111}w_0 - (D^a_{12}+2D^a_{66})d_{122}w_0 \\ &+ F^a_{11}d_{11}\theta_x + F^a_{66}d_{22}\theta_x + (F^a_{12}+F^a_{66})d_{12}\theta_y - A^a_{44}(\theta_x + d_1\theta_z) + Rd_1\theta_z = p_4, \end{aligned} \tag{18d}$$

$$\begin{aligned} &(B^a_{12}+B^a_{66})d_{12}u_0 + B^a_{22}d_{22}v_0 + B^a_{66}d_{11}v_0 - (D^a_{12}+2D^a_{66})d_{112}w_0 - D^a_{22}d_{222}w_0 \\ &+ (F^a_{12}+F^a_{66})d_{12}\theta_x + F^a_{66}d_{11}\theta_y + F^a_{22}d_{22}\theta_y - A^a_{55}(\theta_y + d_2\theta_z) + Rd_2\theta_z = p_5, \end{aligned} \tag{18e}$$

$$\begin{aligned} &L(d_1u_0 + d_2v_0) - L^a(d_{11}w_0 + d_{22}w_0) + (R - A^a_{55})(d_1\theta_x + d_2\theta_y) \\ &+ R^a\theta_z - A^a_{55}(d_{11}\theta_z + d_2\theta_z) = p_6, \end{aligned} \tag{18f}$$

where $\{p\} = \{p_1, p_2, p_3, p_4, p_5, p_6\}^t$ is a generalized force vector, d_{ij}, d_{ijl} and d_{ijlm} are the following differential operators

$$d_{ij} = \frac{\partial^2}{\partial x_i \partial x_j}, \quad d_{ijl} = \frac{\partial^3}{\partial x_i \partial x_j \partial x_l}, \quad d_{ijlm} = \frac{\partial^4}{\partial x_i \partial x_j \partial x_l \partial x_m}, \quad d_i = \frac{\partial}{\partial x_i} \quad (i,j,l,m = 1,2). \tag{19}$$

The components of the generalized force vector $\{p\}$ are given by

$$p_1 = \frac{\partial N^T_x}{\partial x}, \quad p_1 = \frac{\partial N^T_y}{\partial y}, \quad p_3 = q - \frac{\partial^2 M^T_x}{\partial x^2} - \frac{\partial^2 M^T_y}{\partial y^2}, \quad p_4 = \frac{\partial S^T_x}{\partial x}, \quad p_5 = \frac{\partial S^T_y}{\partial y}, \quad P_6 = N^T_z \tag{20}$$

3. Solution procedure

Rectangular plates are generally classified in accordance with the type of support used. We are here concerned with the exact solution of Eqs. (18a-f) for a simply supported FGM plate. The following boundary conditions are imposed at the side edges for the present RHSDT

$$v_0 = w = \theta_y = \theta_z = N_x = M_x = S_x = 0 \quad \text{at} \quad x = 0, a \tag{21a}$$

$$u_0 = w = \theta_x = \theta_z = N_y = M_y = S_y = 0 \quad \text{at} \quad y = 0, b \tag{21b}$$

For TSDT, SSDT, ESDT, HSDT and FSDT, the boundary conditions are

$$v_0 = w = \theta_y = N_x = M_x = S_x = 0 \quad \text{at} \quad x = 0, a \tag{21c}$$

$$u_0 = w = \theta_x = N_y = M_y = S_y = 0 \quad \text{at} \quad y = 0, b \tag{21d}$$

For CPT, the boundary conditions are

$$v_0 = w = N_x = M_x = 0 \quad \text{at} \quad x = 0, a \tag{21e}$$

$$u_0 = w = N_y = M_y = 0 \quad \text{at} \quad y = 0, b \tag{21f}$$

To solve this problem, Navier presented the transverse mechanical and temperature loads q, T_1, T_2, and T_3 in the form of a double trigonometric series as

$$\begin{Bmatrix} q \\ T_1 \\ T_2 \\ T_3 \end{Bmatrix} = \begin{Bmatrix} q_0 \\ t_1 \\ t_2 \\ t_3 \end{Bmatrix} \sin(\lambda x)\sin(\mu y) \tag{22}$$

where q_0, t_1, t_2 and t_3 are constants, $\lambda = \pi / a$, $\mu = \pi / b$.

Following the Navier solution procedure, we assume the following solution form for u_0, v_0, w_0, θ_x, θ_y and θ_z that satisfies the boundary conditions

$$\begin{Bmatrix} u_0 \\ v_0 \\ w_0 \\ \theta_x \\ \theta_y \\ \theta_z \end{Bmatrix} = \begin{Bmatrix} U\cos(\lambda x)\sin(\mu y) \\ V\sin(\lambda x)\cos(\mu y) \\ W\sin(\lambda x)\sin(\mu y) \\ X\cos(\lambda x)\sin(\mu y) \\ Y\sin(\lambda x)\cos(\mu y) \\ Z\sin(\lambda x)\sin(\mu y) \end{Bmatrix}, \tag{23}$$

where U, V, W, X, Y, and Z are arbitrary parameters to be determined subjected to the condition that the solution in Eq. (23) satisfies governing Eqs. (18). One obtains the following operator equation, One obtains the following operator equation

$$[C]\{\Delta\} = \{F\}, \tag{24}$$

where $\{\Delta\} = \{ U, V, W, X, Y, Z\}^t$ and $[C]$ is the symmetric matrix given in Appendix.

In the case of FG plates with various boundary conditions, the present problem can be solved using Ritz method (Uymaz and Aydogdu 2013) or Lévy-type solutions (Ying *et al*. 2009).

4. Numerical results and discussion

The thermomechanical bending analysis is conducted for combinations of metal and ceramic. The set of materials chosen is Titanium and Zirconia. For simplicity, Poisson's ratio of the two materials is assigned the same value (Delale and Erdogan 1983, Bouderba *et al*. 2013). Typical values for metal and ceramics used in the FG sandwich plate are listed in Table 1.

Table 1 Material properties used in the FG sandwich plate

Metal: Ti–6A1–4V	Ceramic: ZrO_2
E_m = 66.2 GPa	E_c = 117.0 GPa
v = 1 / 3	v = 1 / 3
α_m = 10.3 (10^{-6}/K)	α_c = 7.11 (10^{-6}/K)

Table 2 Comparison of dimensionless center deflections $\bar{w}$ for different FG sandwich square plates ($q_0 = t_1 = t_3 = 0$, $t_2 = 100$ and $a / h = 10$)

k	Theory	$\bar{w}$			
		$t_{FGM} / h = 1$	$t_{FGM} / h = 2/3$	$t_{FGM} / h = 1/2$	$t_{FGM} / h = 4/5$
0	Present	0.449863	0.449863	0.449863	0.449863
	Zenkour and Alghamdi (2008)	0.461634	0.461634	0.461634	0.461634
1	Present	0.594840	0.565276	0.542436	0.579538
	Zenkour and Alghamdi (2008)	0.614565	0.586124	0.563416	0.599933
2	Present	0.627934	0.596416	0.567938	0.612832
	Zenkour and Alghamdi (2008)	0.647135	0.618046	0.590491	0.633340
3	Present	0.639690	0.610125	0.579769	0.626505
	Zenkour and Alghamdi (2008)	0.658153	0.631600	0.602744	0.646475
4	Present	0.644833	0.617502	0.586469	0.633395
	Zenkour and Alghamdi (2008)	0.662811	0.638705	0.609560	0.652890
5	Present	0.647421	0.621990	0.590728	0.637353
	Zenkour and Alghamdi (2008)	0.665096	0.642948	0.613842	0.656490

Different dimensionless quantities are used for thermomechanical loading as center deflection

- center deflection $\bar{w} = \dfrac{10^3}{q_0 a^4 / (E_0 h^3) + 10^3 \alpha_0 t_2 \, a^2 / h} w\left(\dfrac{a}{2}, \dfrac{b}{2}\right)$,
- axial stress $\bar{\sigma}_x = \dfrac{10}{q_0 a^2 / h^2 + 10 E_0 \alpha_0 t_2 \, a^2 / h^2} \sigma_x\left(\dfrac{a}{2}, \dfrac{b}{2}, \dfrac{h}{2}\right)$,
- shear stress $\bar{\tau}_{xz} = \dfrac{1}{q_0 a / h + E_0 \alpha_0 t_2 a / (10h)} \tau_{xz}\left(0, \dfrac{b}{2}, 0\right)$.

where the reference values are taken as E_0 = 1 GPa and α_0 = 10^{-6}/K.

In order to prove the validity of the present theory, the dimensionless center deflection $\bar{w}$ presented in Table 2 is compared to that obtained using the method developed by Zenkour and Alghamdi (2008) in the case of thermoelastic loading (q_0 = 0). The present results are in good agreement with other results for all values of the power law index k. Numerical results are tabulated in Tables 3-6 using different plate theories. Additional results are plotted in Figs. 2-8 using the present refined hyperbolic shear deformation theory (RHSDT) with stretching effect ($\varepsilon_z \neq 0$). It is assumed, unless otherwise stated, that $a / h = 10$, $a / b = 1$, $t_1 = 0$, and $q_0 = t_2 = t_3 = 100$. The shear correction factor of FSDT is fixed to be K = 5 / 6.

Table 3 Dimensionless center deflections $\bar{w}$ of the different FG sandwich square plates

k	Theory	$t_{FGM}/h=0$	$t_{FGM}/h=0.2$	$t_{FGM}/h=0.4$	$t_{FGM}/h=0.6$	$t_{FGM}/h=10.8$	$t_{FGM}/h=1$
0	RHSDT	0.771340	0.771340	0.771340	0.771340	0.771340	0.771340
	HSDT	0.817556	0.817556	0.817556	0.817556	0.817556	0.817556
	SSDT	0.796783	0.796783	0.796783	0.796783	0.796783	0.796783
	TSDT	0.808168	0.808168	0.808168	0.808168	0.808168	0.808168
	FSDT	0.895735	0.895735	0.895735	0.895735	0.895735	0.895735
	CPT	0.457873	0.457873	0.457873	0.457873	0.457873	0.457873
1	RHSDT	0.771340	0.841759	0.906271	0.959745	0.999391	1.026070
	HSDT	0.817556	0.896222	0.965660	1.021683	1.062586	1.089928
	SSDT	0.796783	0.873745	0.941636	0.996334	1.036213	1.062840
	TSDT	0.808168	0.886067	0.954808	1.010231	1.050672	1.077690
	FSDT	0.895735	0.979641	1.054630	1.115684	1.160568	1.190728
	CPT	0.457873	0.501163	0.539886	0.571450	0.594688	0.610331
2	RHSDT	0.771340	0.860395	0.943946	1.011993	1.058388	1.084456
	HSDT	0.817556	0.916849	1.006253	1.076785	1.123928	1.150231
	SSDT	0.796783	0.894003	0.981434	1.050237	1.096095	1.121608
	TSDT	0.808168	0.906529	0.995042	1.064791	1.111352	1.137297
	FSDT	0.895735	1.001204	1.097973	1.175402	1.227765	1.257304
	CPT	0.457873	0.512431	0.562536	0.602673	0.629859	0.645223
3	RHSDT	0.771340	0.869136	0.961579	1.035332	1.082231	1.104836
	HSDT	0.817556	0.926476	1.025027	1.101003	1.148302	1.170917
	SSDT	0.796783	0.903467	0.999831	1.073875	1.119794	1.141655
	TSDT	0.808168	0.916083	1.013647	1.088747	1.135420	1.157693
	FSDT	0.895735	1.011279	1.118224	1.202080	1.255041	1.280741
	CPT	0.457873	0.517716	0.573152	0.616662	0.644176	0.657539
4	RHSDT	0.771340	0.874209	0.971671	1.048073	1.094108	1.113637
	HSDT	0.817556	0.932037	1.035690	1.114096	1.160313	1.179771
	SSDT	0.796783	0.908934	1.010269	1.086624	1.131429	1.150192
	TSDT	0.808168	0.921602	1.024208	1.101684	1.147260	1.166403
	FSDT	0.895735	1.017115	1.129824	1.216678	1.268689	1.290961
	CPT	0.457873	0.520783	0.579240	0.624324	0.651345	0.662909
5	RHSDT	0.771340	0.877515	0.978164	1.055935	1.100868	1.118027
	HSDT	0.817556	0.935651	1.042508	1.122124	1.167111	1.184168
	SSDT	0.796783	0.912488	1.016938	1.094427	1.137993	1.154412
	TSDT	0.808168	0.925190	1.030958	1.109609	1.153952	1.170720
	FSDT	0.895735	1.020919	1.137289	1.225706	1.276497	1.296101
	CPT	0.457873	0.522783	0.583160	0.629064	0.655445	0.665606

Table 3 contains the dimensionless center deflection $\bar{w}$ for an FG sandwich plate subjected to mechanical and thermal loads. The deflections are considered for k = 0, 1, 2, 3, 4 and 5 and different FG layer thickness (t_{FGM}). By comparing the results to those obtained by CPT, it can be shown that the effect of shear deformation is to increase the deflection. It can be observed also that the HSDP overestimates the deflections comparatively to RHSDT and this, is due to the thickness stretching effect which is omitted in the theory developed by Atmane *et al*. (2010). For a sandwich plate, the deflections increase with FG layer thickness t_{FGM} and the power law index k.

Table 4 shows the influence of FG layer thickness t_{FGM} on the deflections of FG sandwich plates (k = 3) with different aspect ratio a/b. It can be observed that the deflection increases with the increasing thickness of an FG layer (t_{FGM}) and it is reduced with increasing the aspect ratio a/b. Once again the deflection is increased with including the effect of shear deformation and it is reduced when the thickness stretching effect is taken into consideration ($\varepsilon_z \neq 0$). Tables 5 and 6 list, respectively, the axial stress $\bar{\sigma}_x$ and transverse shear stress $\bar{\tau}_{xz}$ for k = 0, 1, 2, 3, 4 and 5 and different FG layer thickness (t_{FGM}). It can be observed the axial stress $\bar{\sigma}_x$ and transverse shear stress $\bar{\tau}_{xz}$ are very sensitive to the variation of power law index and FG layer thickness. As is observed in the case of deflections, the thickness stretching effect leads also to a reduction of stresses. It can be concluded from Tables 3-6 that the inclusion of thickness stretching effect makes a plate stiffer, and hence, leads to a reduction of deflection and stresses.

Table 4 Effect of aspect ratio a/b on the dimensionless deflection $\bar{w}$ of the FG sandwich plates (k = 3)

t_{FGM}/h	Theory	$a/b=1$	$a/b=2$	$a/b=3$	$a/b=4$	$a/b=5$
0	RHSDT	0.771340	0.300716	0.147654	0.085168	0.054373
	HSDT	0.817556	0.321791	0.159940	0.093790	0.061185
	SSDT	0.796783	0.313432	0.155719	0.091273	0.059512
	TSDT	0.808168	0.318014	0.158033	0.092654	0.060430
	FSDT	0.895735	0.353189	0.175744	0.103172	0.067392
	CPT	0.457873	0.178044	0.088171	0.051659	0.033711
0.2	RHSDT	0.869136	0.338962	0.168161	0.097398	0.062531
	HSDT	0.926476	0.364706	0.181529	0.106696	0.069818
	SSDT	0.903467	0.355510	0.176937	0.104000	0.068059
	TSDT	0.916083	0.360554	0.179457	0.105480	0.069026
	FSDT	1.011279	0.398391	0.198176	0.116327	0.075980
	CPT	0.517716	0.200966	0.099463	0.058261	0.038014
0.4	RHSDT	0.961579	0.374694	0.184359	0.106737	0.068499
	HSDT	1.025027	0.403196	0.200642	0.117924	0.077167
	SSDT	0.999831	0.393146	0.195642	0.115002	0.075273
	TSDT	1.013647	0.398658	0.198386	0.116606	0.076314
	FSDT	1.118224	0.440203	0.218920	0.128491	0.083921
	CPT	0.573152	0.222174	0.109906	0.064364	0.041992

Table 4 Continued

t_{FGM} / h	Theory	a / b = 1	a / b = 2	a / b = 3	a / b = 4	a / b = 5
0.6	RHSDT	1.035332	0.402987	0.198087	0.114556	0.073414
	HSDT	1.101003	0.432682	0.215157	0.126351	0.082600
	SSDT	1.073875	0.421843	0.209748	0.123178	0.080532
	TSDT	1.088747	0.427786	0.212715	0.124919	0.081668
	FSDT	1.202080	0.472957	0.235166	0.138015	0.090138
	CPT	0.616662	0.238790	0.118083	0.069142	0.045106
0.8	RHSDT	1.082229	0.420861	0.206684	0.119392	0.076404
	HSDT	1.148302	0.450940	0.224088	0.131493	0.085879
	SSDT	1.119794	0.439521	0.218366	0.128116	0.083662
	TSDT	1.135420	0.445781	0.221504	0.129968	0.084879
	FSDT	1.255041	0.493613	0.245406	0.144017	0.094055
	CPT	0.644176	0.249267	0.123233	0.072151	0.047066
1	RHSDT	1.104836	0.429399	0.210747	0.121649	0.077765
	HSDT	1.170917	0.459613	0.228305	0.133902	0.087401
	SSDT	1.141655	0.447872	0.222403	0.130406	0.085094
	TSDT	1.157693	0.454308	0.225639	0.132324	0.086360
	FSDT	1.280741	0.503607	0.250355	0.146917	0.095948
	CPT	0.657539	0.254326	0.125715	0.073599	0.048009

Table 5 Dimensionless axial stresses $\bar{\sigma}_x$ of different sandwich square plates

k	Theory	t_{FGM} / h = 0	t_{FGM} / h = 0.2	t_{FGM} / h = 0.4	t_{FGM} / h = 0.6	t_{FGM} / h = 0.8	t_{FGM} / h = 1
0	RHSDT	-1.650736	-1.650736	-1.650736	-1.650736	-1.650736	-1.650736
	HSDT	-2.523043	-2.523043	-2.523043	-2.523043	-2.523043	-2.523043
	SSDT	-2.388919	-2.388919	-2.388919	-2.388919	-2.388919	-2.388919
	TSDT	-2.461177	-2.461177	-2.461177	-2.461177	-2.461177	-2.461177
	FSDT	-3.597007	-3.597007	-3.597007	-3.597007	-3.597007	-3.597007
	CPT	-1.706393	-1.706393	-1.706393	-1.706393	-1.706393	-1.706393
1	RHSDT	-1.650736	-3.372080	-2.859305	-2.461461	-2.179138	-1.993540
	HSDT	-2.523050	-3.480127	-3.140399	-2.865768	-2.665136	-2.531150
	SSDT	-2.388919	-3.333300	-3.001265	-2.733086	-2.537374	-2.406806
	TSDT	-2.461177	-3.412724	-3.076466	-2.804750	-2.606343	-2.473903
	FSDT	-3.597007	-4.504051	-4.136892	-3.838047	-3.618476	-3.471099
	CPT	-1.706393	-2.193219	-2.003463	-1.848793	-1.734921	-1.658265
2	RHSDT	-1.650736	-3.211762	-2.556774	-2.066031	-1.751165	-1.580468
	HSDT	-2.523050	-3.379455	-2.941822	-2.595856	-2.364496	-2.235677

Table 5 Continued

k	Theory	$t_{FGM}/h=0$	$t_{FGM}/h=0.2$	$t_{FGM}/h=0.4$	$t_{FGM}/h=0.6$	$t_{FGM}/h=0.8$	$t_{FGM}/h=1$
2	SSDT	-2.388919	-3.234499	-2.806645	-2.469045	-2.243809	-2.118730
	TSDT	-2.461177	-3.312889	-2.879670	-2.537489	-2.308903	-2.181780
	FSDT	-3.597007	-4.398484	-3.924721	-3.545789	-3.289757	-3.145662
	CPT	-1.706393	-2.137999	-1.892474	-1.695789	-1.562571	-1.487285
3	RHSDT	-1.650736	-3.137344	-2.419727	-1.898185	-1.588667	-1.446122
	HSDT	-2.523050	-3.332439	-2.849905	-2.477118	-2.244947	-2.134330
	SSDT	-2.388919	-3.188312	-2.716593	-2.353122	-2.127496	-2.020425
	TSDT	-2.461177	-3.266245	-2.788595	-2.420027	-2.190823	-2.081815
	FSDT	-3.597007	-4.349165	-3.825600	-3.415261	-3.156414	-3.031283
	CPT	-1.706393	-2.112102	-1.840454	-1.627241	-1.492417	-1.426935
4	RHSDT	-1.650736	-3.094600	-2.343139	-1.809688	-1.511078	-1.390767
	HSDT	-2.523050	-3.305276	-2.797679	-2.412894	-2.186019	-2.091004
	SSDT	-2.388919	-3.161620	-2.665468	-2.290552	-2.070361	-1.978602
	TSDT	-2.461177	-3.239292	-2.736867	-2.356554	-2.132710	-2.039172
	FSDT	-3.597007	-4.320597	-3.768831	-3.343853	-3.089733	-2.981507
	CPT	-1.706393	-2.097076	-1.810621	-1.589696	-1.457288	-1.400620
5	RHSDT	-1.650736	-3.066950	-2.294758	-1.756372	-1.468147	-1.446122
	HSDT	-2.523050	-3.287616	-2.764272	-2.373503	-2.152668	-2.069541
	SSDT	-2.388919	-3.144264	-2.632792	-2.252244	-2.038118	-1.957968
	TSDT	-2.461177	-3.221769	-2.703791	-2.317655	-2.099863	-2.018086
	FSDT	-3.597007	-4.301976	-3.732298	-3.299697	-3.051612	-2.956534
	CPT	-1.706393	-2.087272	-1.791409	-1.566468	-1.437193	-1.387402

Table 6 Dimensionless transverse shear stresses $\bar{\tau}_{xz}$ of different sandwich square plates

k	Theory	$t_{FGM}/h=0$	$t_{FGM}/h=0.2$	$t_{FGM}/h=0.4$	$t_{FGM}/h=0.6$	$t_{FGM}/h=0.8$	$t_{FGM}/h=1$
0	RHSDT	0.142427	0.142427	0.142427	0.142427	0.142427	0.142427
	HSDT	0.175814	0.175814	0.175814	0.175814	0.175814	0.175814
	SSDT	0.171604	0.171604	0.171604	0.171604	0.171604	0.171604
	TSDT	0.174481	0.174481	0.174481	0.174481	0.174481	0.174481
	FSDT	0.173624	0.173624	0.173624	0.173624	0.173624	0.173624
1	RHSDT	0.142427	0.245892	0.271139	0.263095	0.250022	0.245207
	HSDT	0.175814	0.258120	0.280007	0.275689	0.267830	0.267638
	SSDT	0.171604	0.271618	0.300347	0.293865	0.280890	0.277019
	TSDT	0.174481	0.264677	0.289538	0.284236	0.274133	0.272347
	FSDT	0.173624	0.181504	0.190134	0.199626	0.210115	0.221768

Table 6 Continued

k	Theory	$t_{FGM}/h=0$	$t_{FGM}/h=0.2$	$t_{FGM}/h=0.4$	$t_{FGM}/h=0.6$	$t_{FGM}/h=0.8$	$t_{FGM}/h=1$
	RHSDT	0.142427	0.266548	0.287198	0.265886	0.243455	0.239333
	HSDT	0.175814	0.274559	0.293708	0.279786	0.265773	0.268627
2	SSDT	0.171604	0.292205	0.317892	0.298078	0.275130	0.272583
	TSDT	0.174481	0.282950	0.304910	0.288355	0.270427	0.270952
	FSDT	0.173624	0.184293	0.196359	0.210115	0.225945	0.244354
	RHSDT	0.142427	0.274786	0.290668	0.261357	0.235362	0.235593
	HSDT	0.175814	0.281176	0.297080	0.277265	0.261228	0.269434
3	SSDT	0.171604	0.300600	0.322239	0.294047	0.267073	0.269608
	TSDT	0.174481	0.290349	0.308697	0.285154	0.264327	0.270110
	FSDT	0.173624	0.185719	0.199626	0.215785	0.234789	0.257465
	RHSDT	0.142427	0.279028	0.291316	0.257131	0.230171	0.235324
	HSDT	0.175814	0.284630	0.298000	0.274576	0.258355	0.272013
4	SSDT	0.171604	0.305016	0.323396	0.289951	0.261729	0.270017
	TSDT	0.174481	0.294226	0.309711	0.281837	0.260366	0.271755
	FSDT	0.173624	0.186586	0.201639	0.219335	0.240436	0.266029
	RHSDT	0.142427	0.281670	0.291163	0.253889	0.227025	0.236707
	HSDT	0.175814	0.286716	0.298171	0.272440	0.256771	0.275287
5	SSDT	0.171604	0.307694	0.323573	0.286687	0.258433	0.272071
	TSDT	0.174481	0.296571	0.309879	0.279200	0.258029	0.274512
	FSDT	0.173624	0.187168	0.203004	0.221768	0.244354	0.272062

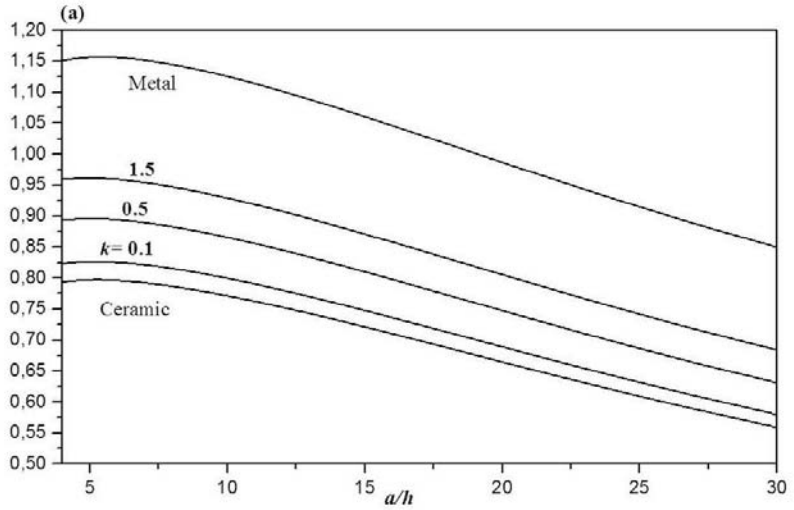

Fig. 2 Dimensionless center deflection $\bar{w}$ as a function of side-to-thickness ratio a/h for two types of sandwich plates: (a) $t_{FGM}=0.4h$; (b) $t_{FGM}=0.8$

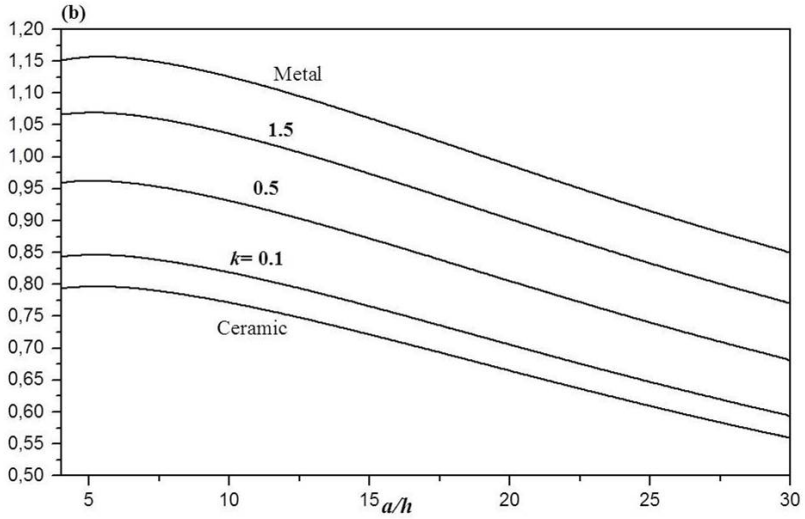

Fig. 2 Continued

Fig. 2 shows the variation of the center deflection $\bar{w}$ with side-to-thickness ratio a/h for two types of sandwich plates with different FGM layer thickness (t_{FGM}). The deflection of the metallic plate is found to be the largest magnitude and that of the ceramic plate of the smallest magnitude. The deflections of the FG sandwich and homogeneous plates decrease as a/h increases. It is to be noted that the FG sandwich plates with intermediate properties undergo corresponding intermediate values of center deflection. This is expected because the metallic plate is the one with the lowest stiffness and the ceramic plate is the one with the highest stiffness.

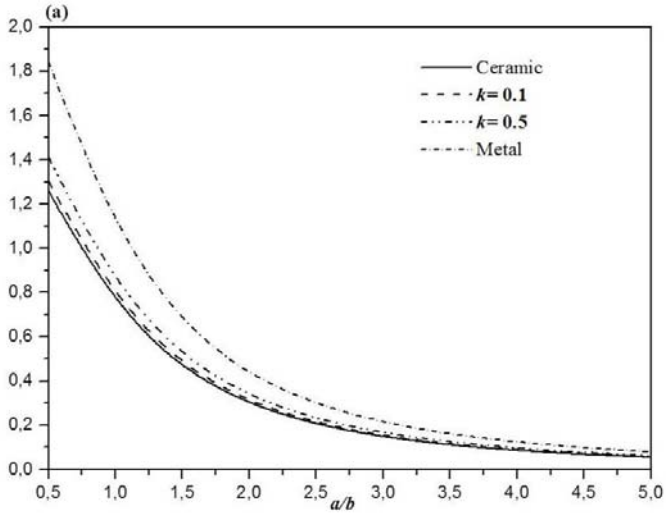

Fig. 3 Effect of the aspect ratio a/b on dimensionless center deflection $\bar{w}$ for two types of sandwich plates: (a) $t_{FGM} = 0.4h$; (b) $t_{FGM} = 0.8$

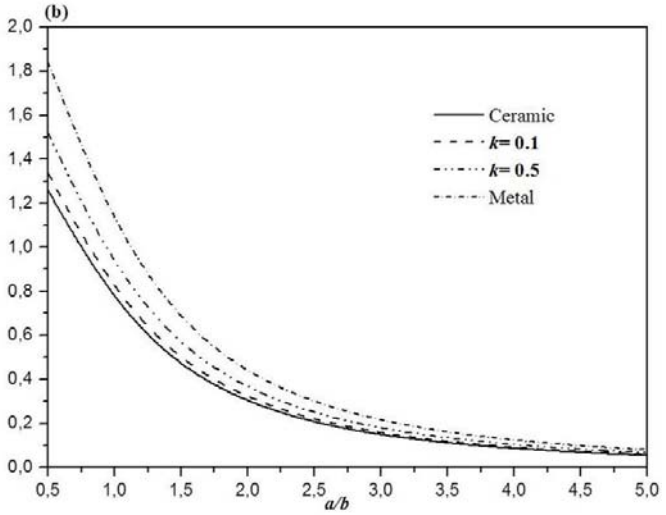

Fig. 3 Continued

Fig. 3 shows the effects of the aspect ratio a / b on the dimensionless deflection $\bar{w}$. The deflection of the ceramic plate is found to be of the smallest magnitude and that of the metallic plate, of the largest magnitude. The increase of the aspect ratio a / b leads to a decrease of deflections of the homogeneous and FG sandwich plates. It is to be noted that the FG sandwich plates with intermediate properties undergo corresponding intermediate values of center deflection.

Fig. 4 shows the variation of axial stress $\bar{\sigma}_x$ through-the thickness of the homogeneous ceramic and FG sandwich plates. The stresses are tensile below the mid-plane and compressive above the

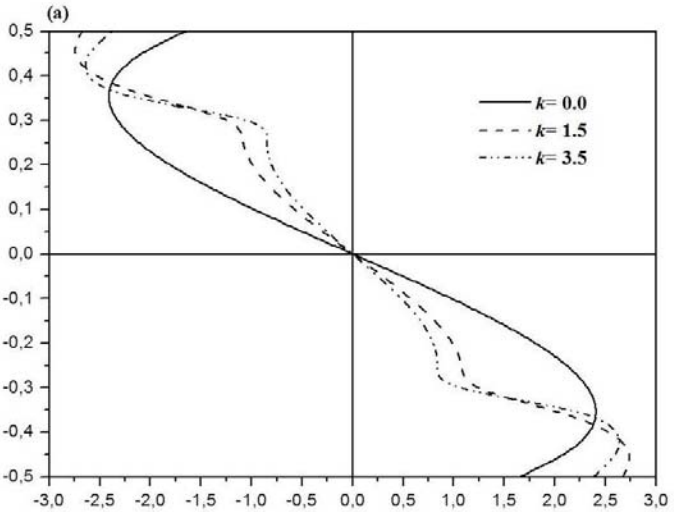

Fig. 4 Variation of axial stress $\bar{\sigma}_x$ through the plate thickness for two types of sandwich plates: (a) $t_{FGM} = 0.4h$; (b) $t_{FGM} = 0.8$

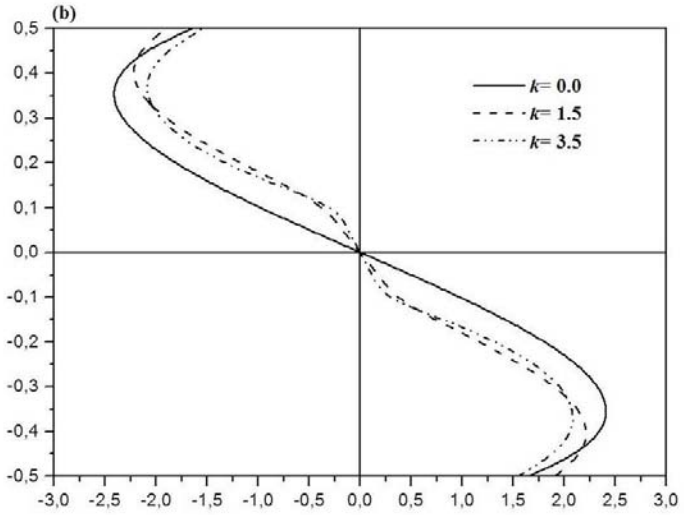

Fig. 4 Continued

mid-plane. As expected, the different volume fraction exponents influences considerably the variation of axial stresses.

Fig. 5 shows plots of the through-the-thickness distribution of the transverse shear stress $\overline{\tau}_{xz}$ for k = 0.0, 1.5, and 3.5. The maximum value occurs at a point on the mid-plane of the plate and its magnitude for FG plate is larger than that for homogeneous ceramic plate.

Fig. 6 shows the effect of the aspect ratio a/b on the dimensionless center deflection $\overline{w}$ for FG

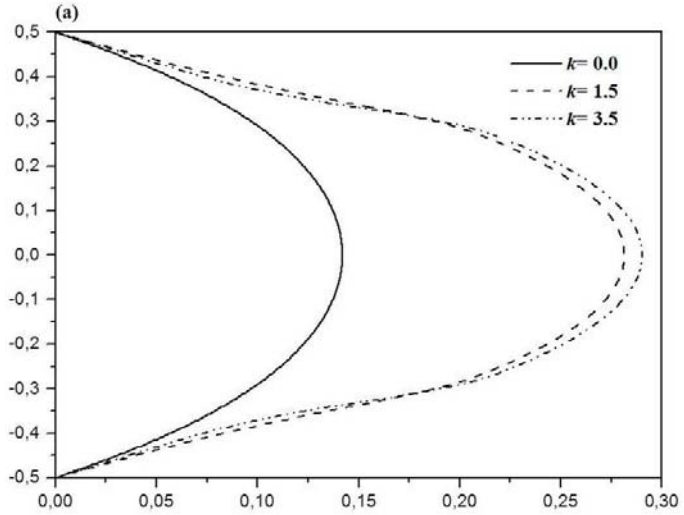

Fig. 5 Variation of transverse shear stress $\overline{\tau}_{xz}$ through the plate thickness for two types of sandwich plates: (a) $t_{FGM} = 0.4h$; (b) $t_{FGM} = 0.8$

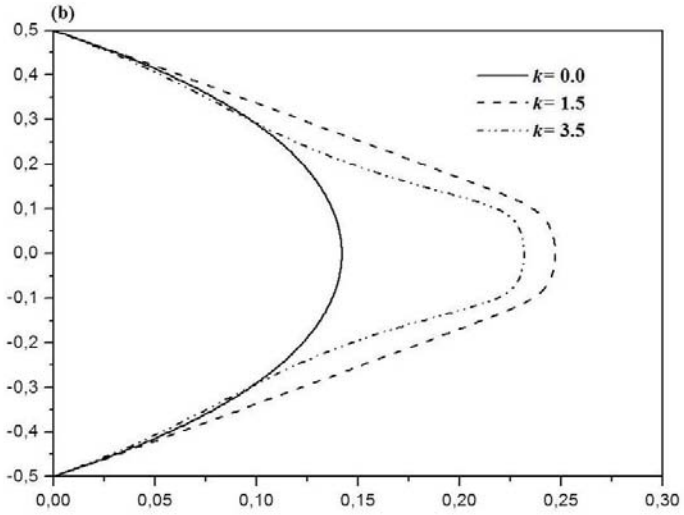

Fig. 5 Continued

sandwich plate. The effect of the mechanical and thermal loads is taken into consideration. It is found that the aspect ratio effect is more pronounced on the thermomechanical bending deflection $\overline{w}$ ($q_0 = t_2 = t_3 = 100$ and) of the FG sandwich plate.

In Figs. 7 and 8, we have plotted the through-the-thickness distributions of the dimensionless axial stress $\overline{\sigma}_x$ and the transverse shear stress $\overline{\tau}_{xz}$ of the FG sandwich plate for $k = 3.5$ and $t_{FGM} = 0.4h$, respectively. These figures show the great influence played by the different thermal and bending loads on the axial and transverse shear stresses.

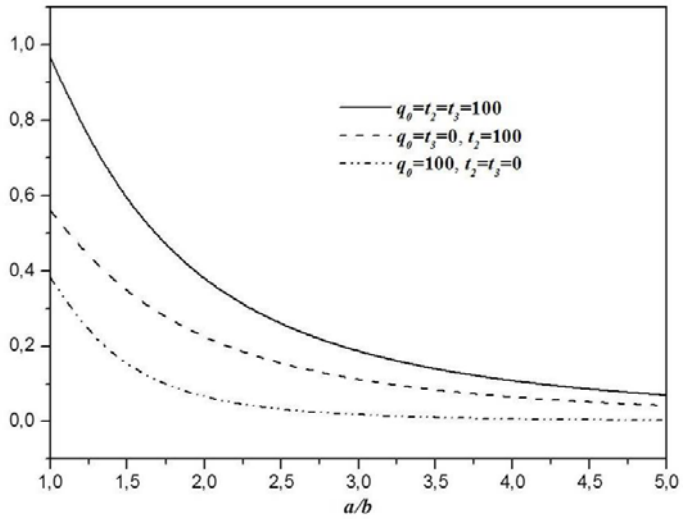

Fig. 6 Effect of mechanical and temperature loads on the dimensionless center deflection of FG sandwich plate versus a / b ($t_{FGM} = 0.4h$, $k = 3.5$).

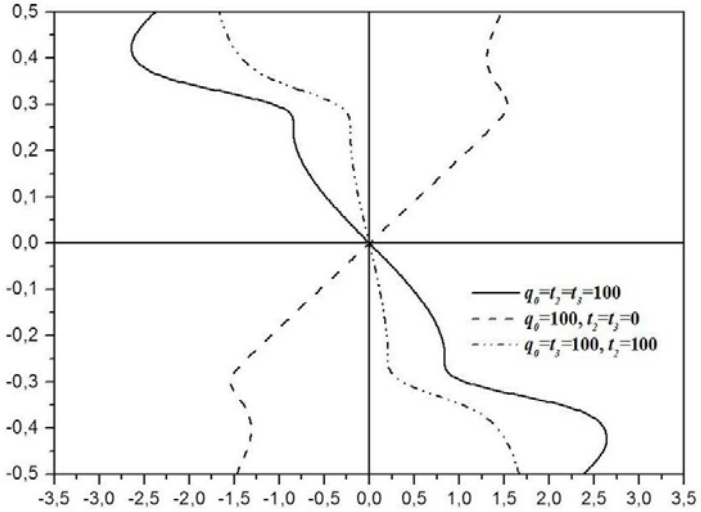

Fig. 7 Effect of mechanical and temperature loads on the dimensionless axial stress of FG sandwich plate ($t_{FGM} = 0.4h$, $k = 3.5$)

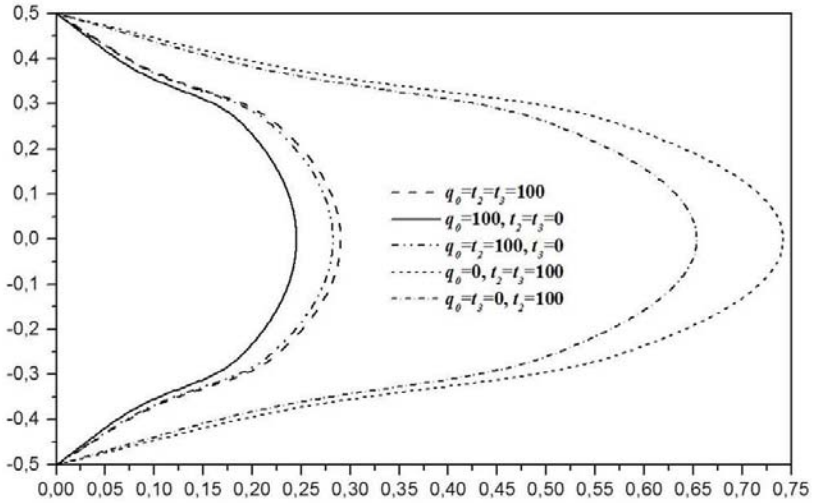

Fig. 8 Effect of mechanical and temperature loads on the dimensionless transverse shear stress of FG sandwich plate ($t_{FGM} = 0.4h$, $k = 3.5$)

5. Conclusions

A novel hyperbolic shear deformation theory for thermomechanical bending of FG sandwich plates is presented. The theory accounts for the stretching and shear deformation effects without requiring a shear correction factor. The gradation of properties through the thickness is assumed to be of the power law type and comparisons have been made with homogeneous isotropic plates. Numerical results for stresses and deflection are obtained and investigated for different plate

configurations. It has been confirmed that the inclusion of thickness stretching effect makes a plate stiffer, and hence, leads to a reduction of deflections and stresses.

References

Abdelaziz, H.H., Atmane, H.A., Mechab, I., Boumia, L., Tounsi, A. and Adda Bedia, E.A. (2011), "Static analysis of functionally graded sandwich plates using an efficient and simple refined theory", *Chinese J. Aeronaut.*, **24**(4), 434-448.

Atmane, H.A., Tounsi, A., Mechab, I. and Adda Bedia, E.A. (2010), "Free vibration analysis of functionally graded plates resting on Winkler–Pasternak elastic foundations using a new shear deformation theory", *Int. J. Mech. Mater. in Design*, **6**(2), 113-121.

Bert, C.W. (1984), "A critical evaluation of new plate theories applied to laminated composites", *Compos. Struct.*, **2**(4), 794-805.

Bian, Z.G., Chen, W.Q., Lim, C.W. and Zhang, N. (2005), "Analytical solutions for single- and multi-span functionally graded plates in cylindrical bending", *Int. J. Solid. Struct.*, **42**(24-25), 6433-6456.

Bouderba, B., Houari, M.S.A. and Tounsi, A. (2013), "Thermomechanical bending response of FGM thick plates resting on Winkler-Pasternak elastic foundations", *Steel Compos. Struct.*, *Int. J.*, **14**(1), 85-104.

Bourada, M., Tounsi, A., Houari, M.S.A. and Adda Bedia, E.A. (2012), "A new four-variable refined plate theory for thermal buckling analysis of functionally graded sandwich plates", *J. Sandwich Struct. Mater.*, **14**(1), 5-33.

Cheng, Z.Q. and Batra, R.C. (2000a), "Deflection relationships between the homogeneous kirchhoff plate theory and different functionally graded plate theories", *Arch. Mech.*, **52**(1), 143-158.

Cheng, Z.Q. and Batra, R.C. (2000b), "Exact correspondence between eigenvalues of membranes and functionally graded simply supported polygonal plates", *J. Sound Vib.*, **229**(4), 879-895.

Cheng, Z.Q. and Batra, R.C. (2000c), "Three-dimensional thermoelastic deformations of a functionally graded elliptic plate", *Compos. Part B: Eng.*, **31**(2), 97-106.

Delale, F. and Erdogan, F. (1983), "The crack problem for a nonhomogeneous plane", *J. Appl. Mech.*, **50**(3), 609-614.

Hadji, L., Atmane, H.A., Tounsi, A., Mechab, I. and Adda Bedia, E.A. (2011), "Free vibration of functionally graded sandwich plates using four variable refined plate theory", *Applied Mathematics and Mechanics*, **32**(7), 925-942.

Hamidi, A., Zidi, M., Houari, M.S.A. and Tounsi, A. (2013), "A new four variable refined plate theory for bending response of functionally graded sandwich plates under thermomechanical loading", *Compos. Part B:Eng.* (In press).

Houari, M.S.A, Benyoucef, S., Mechab, I., Tounsi, A. and Adda bedia, E.A. (2011), "Two variable refined plate theory for thermoelastic bending analysis of functionally graded sandwich plates", *J. Thermal Stresses*, **34**(4), 315-334.

Karama, M., Afaq, K.S. and Mistou, S. (2003), "Mechanical behavior of laminated composite beam by the new multilayered laminated composite structures model with transverse shear stress continuity", *Int. J. Solid. Struct.*, **40**(6), 1525-1546.

Levinson, M. (1980), "An accurate simple theory of the statics and dynamics of elastic plates", *Mech. Res. Commun.*, **7**, 343-350.

Lim, C.W., Yang, Q. and Lü, C.F. (2009), "Two-dimensional elasticity solutions for temperature-dependent in-plane vibration of FGM circular arches", *Compos. Struct.*, **90**(3), 323-329.

Lo, K.H., Chiristensen, R.M. and Wu, E.M. (1977), "A higher-order theory of plate deformation, part 2: laminated plates", *J. Appl. Mech.*, **44**(4), 669-676.

Lü, C.F., Lim, C.W. and Chen, W.Q. (2009a), "Semi-analytical analysis for multi-directional functionally graded plates: 3-D elasticity solutions", *Int. J. Numer. Method. Eng.*, **79**(1), 25-44.

Lü, C.F., Lim, C.W. and Chen, W.Q. (2009b), "Exact solutions for free vibrations of functionally graded

thick plates on elastic foundations", *Mech. Adv. Mater. Struct.*, **16**(8), 576-584.
Matsunaga, H. (2000), "Vibration and stability of cross-ply laminated composite plates according to a global higher-order plate theory", *Compos. Struct.*, **48**(4), 231-244.
Matsunaga, H. (2009), "Thermal buckling of functionally graded plates according to a 2 D higher-order deformation theory", *Compos. Struct.*, **90**(1), 76-86.
Merdaci, S., Tounsi, A., Houari, M.S.A., Mechab, I., Hebali, H. and Benyoucef, S. (2011), "Two new refined shear displacement models for functionally graded sandwich plates", *Arch. Appl. Mech.*, **81**(11), 1507-1522.
Mindlin, R.D. (1951), "Influence of rotatory inertia and shear on flexural vibrations of isotropic elastic plates", *J. Appl. Mech.*, **73**, 31-38.
Murthy, M.V. (1981), "An improved transverse shear deformation theory for laminated anisotropic plates", NASA Technical Paper 1903.
Reddy, J.N. (1984), "A simple higher-order theory for laminated composite plates", *J. Appl. Mech.*, **51**(4), 745-752.
Reddy, J.N. (2000), "Analysis of functionally graded plates", *Int. J. Num. Method. Eng.*, **47**(1-3), 663-684.
Reissner, E. (1945), "The Effect of transverse shear deformation on the bending of elastic plates", *J. Appl. Mech.*, **12**, 69-77.
Şimşek, M. (2009), Static analysis of a functionally graded beam under a uniformly distributed load by Ritz method, *Int. J. Eng. Appl. Sci.*, **1**(3), 1-11.
Şimşek, M. (2010), "Vibration analysis of a functionally graded beam under a moving mass by using different beam theories", *Compos. Struct.*, **92**(4), 904-917.
Tounsi, A., Houari, M.S.A., Benyoucef, S. and Adda Bedia, E.A. (2013), "A refined trigonometric shear deformation theory for thermoelastic bending of functionally graded sandwich plates", *Aerosp. Sci. Tech.*, **24**(1), 209-220.
Uymaz, B. and Aydogdu, M. (2013), "Three dimensional shear buckling of FG plates with various boundary conditions", *Composite Structures*, **96**, 670-682.
Vel, S.S. and Batra, R.C. (2002), "Exact Solution for Thermoelastic Deformations of Functionally Graded Thick Rectangular Plates", *AIAA J.*, **40**(7), 1421-1433.
Yaghoobi, H. and Yaghoobi, P. (2013), "Buckling analysis of sandwich plates with FGM face sheets resting on elastic foundation with various boundary conditions: An analytical approach", *Meccanica*, March. (In press).
Ying, J., Lü, C.F. and Lim, C.W. (2009), "3D thermoelasticity solutions for functionally graded thick plates", *J Zhejiang Univ Sci A*, **10**(3), 327-336.
Zhang, X.Z., Kitipornchai, S., Liew, K.M., Lim, C.W. and Peng, L.X. (2003), "Thermal stresses around a circular hole in a functionally graded plate", *J. Therm. Stresses*, **26**(4), 379-390.
Zenkour, A.M. and Alghamdi, N. (2008), "Thermoelastic bending analysis of functionally graded sandwich plates", *J. Mater. Sci.*, **43**(8), 2574-2589.
Zenkour, A.M. and Alghamdi, N. (2010), "Bending analysis of functionally graded sandwich plates under the effect of mechanical and thermal loads", *Mech. Adv. Mater. Struct.*, **17**(6), 419-432.
Zeng, Q.C., Lim, C.W., Lü, C.F. and Yang, Q. (2012), "Asymptotic two-dimensional elasticity approach for free vibration of FGM circular arches", *Mech. Adv. Mater. Struct.*, **19**(1-3), 29-38.

CC

Appendix

The stiffness coefficients C_{ij} of the symmetric matrix $[C]$ appeared in Eq. (24) are as follows

$$
\begin{aligned}
C_{11} &= -\left(A_{11}\lambda^2 + A_{66}\mu^2\right), \\
C_{22} &= -\lambda\,\mu\left(A_{12} + A_{66}\right), \\
C_{13} &= \lambda\left[B_{11}\lambda^2 + \left(B_{12} + 2B_{66}\right)\mu^2\right], \\
C_{14} &= -\left(B_{11}^a\lambda^2 + B_{66}^a\mu^2\right), \\
C_{15} &= -\left(B_{12}^a + B_{66}^a\right)\lambda\,\mu, \\
C_{16} &= \lambda\,L, \\
C_{22} &= -\left(A_{66}\lambda^2 + A_{22}\mu^2\right), \\
C_{23} &= \mu\left[\left(B_{12} + 2B_{66}\right)\lambda^2 + B_{22}\mu^2\right], \\
C_{24} &= C_{15}, \\
C_{25} &= -\left(B_{66}^a\lambda^2 + B_{22}^a\mu^2\right), \\
C_{26} &= \mu\,L, \\
C_{33} &- \left[D_{11}\lambda^4 + 2\left(D_{12} + 2D_{66}\right)\lambda^2\mu^2 + D_{22}\mu^4\right], \\
C_{34} &= \lambda\left[D_{11}^a\lambda^2 + \left(D_{12}^a + 2D_{66}^a\right)\mu^2\right], \\
C_{35} &= \mu\left[\left(D_{12}^a + 2D_{66}^a\right)\lambda^2 + D_{22}^a\mu^2\right], \\
C_{36} &= -L^a\left(\lambda^2 + \mu^2\right), \\
C_{44} &= -\left[F_{11}^a\lambda^2 + F_{66}^a\mu^2 + A_{44}^a\right], \\
C_{45} &= -\lambda\,\mu\left(F_{12}^a + F_{66}^a\right), \\
C_{46} &= \lambda\left(R - A_{44}^a\right), \\
C_{55} &= -\left[F_{66}^a\lambda^2 + F_{22}^a\mu^2 + A_{55}^a\right], \\
C_{56} &= \mu\left(R - A_{55}^a\right), \\
C_{66} &= -\left[\lambda^2 A_{44}^a + \mu^2 A_{55}^a + R^a\right].
\end{aligned}
$$

The components of the generalized force vector $\{F\} = \{F_1, F_2, F_3, F_4, F_5\}^t$ are given by

$$
\begin{aligned}
F_1 &= \lambda\left(A^T t_1 + B^T t_2 + B_a^T t_3\right), \\
F_2 &= \mu\left(A^T t_1 + B^T t_2 + B_a^T t_3\right), \\
F_3 &= -q_0 - h\left(\lambda^2 + \mu^2\right)\left[B^T t_1 + D^T t_2 + D_a^T t_3\right], \\
F_4 &= \lambda\, h\left(B_a^T t_1 + D_a^T t_2 + F_a^T t_3\right), \\
F_5 &= \mu\, h\left(B_a^T t_1 + D_a^T t_2 + F_a^T t_3\right), \\
F_6 &= \; -h\left(L^T t_1 + L_a^T t_2 + R^T t_3\right).
\end{aligned}
$$

where

$$\left(A^T, B^T, D^T\right) = \sum_{n=1}^{3} \int_{h_n}^{h_{n+1}} \frac{E(z)}{1-\nu^2}\left(1+2\ \nu\right) \alpha\alpha(z\left(1, \bar{z}, \bar{z}^2\right) dz,$$

$$\left(B_a^T, D_a^T, F_a^T\right) = \sum_{n=1}^{3} \int_{h_n}^{h_{n+1}} \frac{E(z)}{1-\nu^2}\left(1+2\ \nu\right) \alpha\alpha(z\bar{f}(z)\ \left(1, \bar{z}, \bar{f}\right) dz,$$

$$\left(L^T, L_a^T, R^T\right) = \sum_{n=1}^{3} \int_{h_n}^{h_{n+1}} \frac{E(z)}{1-\nu^2}\left(1+2\,\nu\right) \alpha(z)\ \bar{f}''(z)\ \left(1, \bar{z}, \bar{f}\right) dz,$$

in which $\bar{z} = z/h$, $\bar{f}(z) = f(z)/h$ and $\bar{f}''(z) = f''(z)/h$.